Geotechnical Safety and Risk V
T. Schweckendiek et al. (Eds.)

doi:10.3233/978-1-61499-580-7-431

Calibration of Partial Factors for Basal Reinforced Piled Embankments

P.G. VAN DUIJNEN [a] , T. SCHWECKENDIEK [b,c] , E.O.F. CALLE [b] , S.J.M. VAN EEKELEN [b,c]
[a] *HUESKER Synthetic BV, Netherlands*
[b] *Deltares, Netherlands*
[c] *Delft university of technology, Netherlands*

Abstract. In the Netherlands, the design guideline for basal reinforced piled embankments has been revised (CUR226:2015) adopting a new analytical design model (The Concentric Arches (CA) model, Van Eekelen et al., 2013; 2015). The CA model provides geosynthetic reinforcement (GR) strains which were compared with laboratory and in situ measurements (Van Eekelen et al., 2015). The corresponding discrepancies between the measured values and the values calculated with the new model have been assessed statistically in order to obtain model error statistics as suggested in Eurocode: basis of design (NEN, 2011). Monte Carlo (MC) simulations were carried out to obtain model, material and load factors using several reference cases, in order to calibrate the semi-probabilistic design approach for the revised Dutch Design guideline for Piled Embankments (CUR226, 2015). This paper discusses both the assessment of the model error as well as the calibration of the partial factors, including the lessons learnt.

Keywords. Monte Carlo (MC) analyses, partial factors, piled embankments, model error, code calibration, geosynthetics

1. Introduction

A major challenge for technical committees in generating design guidelines and codes of practice is the choice of safety levels achieved by prescribing partial safety factors. The method must provide sufficient reliability, yet at the same time the resulting design should be economic. The Dutch CUR-Committee for piled embankments chose a probabilistic approach to determine the partial factors in order to follow a rational and objective procedure. Table 1 lists the five main procedure steps discussed in this paper.

Table 1. Process steps calibrating partial factors

Step	Phase description
1	Define the failure mechanisms.
2	Compare model calculations with measured data.
3	Perform reliability analyses for reference cases.
4	Calibration of the model factor.
5	Calibration of the partial load and material factors.

Before discussing all steps in detail, the piled embankment concept is explained.

2. Piled Embankment

2.1. What is a Piled Embankment?

A basal reinforced piled embankment is constructed to build roads, railways or platforms in soft soil areas. They are constructed relatively quickly, settlement-free and they do not damage adjacent sensitive constructions by horizontal soil deformations. A basal reinforced piled embankment consists of (bottom-up in Figure 1):

- a foundation of piles with (or sometimes without) pile caps.
- geosynthetic reinforcement (GR). This is the basal reinforcement, installed in one or more layers.
- an embankment. The bottom layer of the embankment (the 'mattress') must consist of a frictional material, like sand or crushed aggregate (e.g. crushed rock or crushed recycled construction material).

The load transferred to the pile caps is partly due to arching and partly transferred through the GR. The 2015 update of the Dutch CUR226 guideline for the design of basal reinforced piled

embankments adopted a new model for the GR design: the Concentric Arches (CA) model of Van Eekelen et al., (2013; 2015, Figure 1). This CA model calculates a value for the maximum GR strain and corresponding tensile force in two calculation steps.

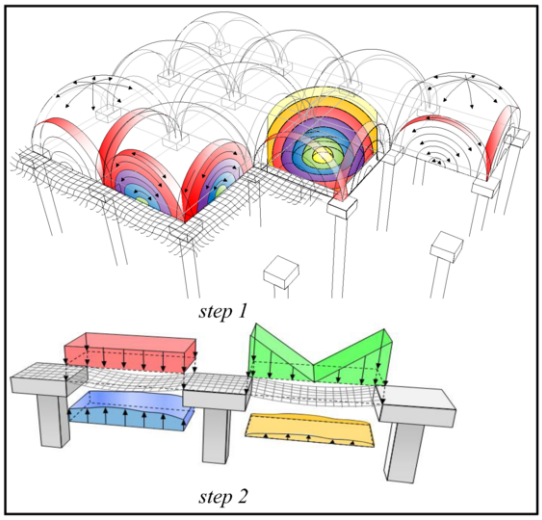

Figure 1. The Concentric Arches model for GR design in a basal reinforced piled embankment (Van Eekelen et al., 2013 and 2015) (*step 1*) the load is transferred along the 3D and 2D arches, (*step 2*) the GR strain and tensile force is calculated in the GR strips between adjacent piles

2.2. Why a new method?

Van Eekelen et al. (2015) showed that the new CA model, adopted in CUR226 (2015), calculates GR strains that are on average 1.06 times higher than the values measured in seven full-scale projects and four series of scaled model experiments, while the model of the old version of CUR226 (2010) calculated GR strains that were on average 2.46 times higher than the measured values. Although the standard deviation was also reduced with the new model, a considerable standard deviation remained.

3. Step 1: Failure Mechanisms

3.1. System Reliability

Eurocode 0 (EC1990) provides target reliability indices β (or equivalently, target probabilities of failure P_f) for each consequence class (CC) or reliability class (RC). For the Dutch piled embankment guideline, these target values were interpreted to refer to the entire structural system, consisting of several failure mechanisms such as (1) structural failure of the pile cap, (2) bearing capacity failure of the piles, (3) fracture of the GR, (4) slip surface instability of the total system. The last failure mechanism is not realistic in most cases.

3.2. Fault tree

The simplified fault tree in Figure 2 visualizes the most relevant failure mechanisms for a piled embankment system.

The total system failure probability depends on the interaction between individual mechanisms. For example: The bearing capacity is determined by both the pile bearing capacity and the soil between piles. Other mechanisms like fracture of the reinforcement or loss of bearing capacity result directly in total system failure. In that case, the upper bound of the system failure probability is the sum of individual failure mechanism (an OR-gate $\oplus$).

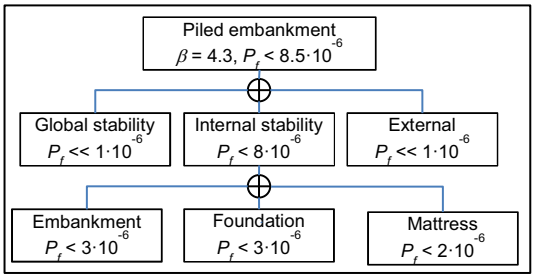

Figure 2. Tree of failure mechanisms (RC3).

3.3. Target probabilities per failure mechanism

Target probabilities of failure can be assigned to individual failure mechanisms, based on their role in the system as defined by the fault tree (see e.g. Schweckendiek et al., 2012). For design situations, the allocation of target probabilities of failure is largely arbitrary as long as the overall system target reliability is met. It makes sense to allocate rather high target values to failure mechanisms for which the mitigation is rather costly. The failure tree for all three reliability classes is defined and used in the MC analysis.

4. Step 2: Comparing Model Calculations with Measured Data

4.1. Collecting Data

Van Eekelen et al. (2015) collected 11 experimental and field test series and compared measured GR strains with values calculated with the new CA model, which was adopted in the CUR226 (2015) guideline. This resulted in 122 data points. Seven of these points were rejected as the polypropylene (PP) reinforcement crept too much during the experiment. The data set is described in detail in Van Eekelen et al. (2015).

4.2. Assessment of Model Error

Figure 3 shows the ratio between measured GR strains r_e and calculated GR strains r_f for the 115 relevant experiments. For 22 data points, the calculations gave an under-prediction of the measured strains (r_e/r_t > 1.0) and for the remaining 93 an over-prediction ($r_e/r_t \leq 1.0$, i.e. conservative behaviour of the model). The mean model bias, assessed as suggested in Eurocode 0 (annex D), is 0.727 and the variation of the error terms is about 0.702. Table 4 presents more detailed information for several sub-sets of data.

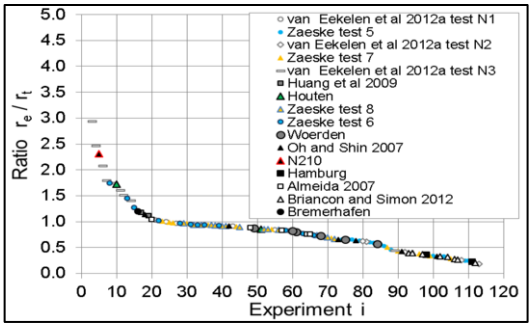

Figure 3. Ratio of measured GR strain (r_e) and calculated GR strain (r_t), sorted in descending order. Two results (ratios > 5-8) are beyond the displayed scale. Data obtained from Van Eekelen et al. (2015).

5. Step 3: Reliability Analyses for Reference Cases

5.1. Geometry

The coefficient of variation of the pile centre-to-centre distance was determined by analysing the measured pile position for a project in Houten (Van Duijnen et al., 2010). The result is given in Table 2.

5.2. Material Properties Embankment Fill

In the Netherlands, the default values for the coefficient of variation (V) of common soil types are stated in the national annex of EC7. Table 2 presents the values used in the present study.

For the soil properties, the student-T distribution for the 95% value is used.

$$x_{ave,p} = \bar{X} - t_{N-1}^{p} \cdot \frac{s_x}{\sqrt{N}} \qquad (1)$$

Table 2. Coefficients of variation of soil properties and geometry as applied in the calibration study

Property	V
Centre-to-centre distance	0.10 m
Embankment height	0.05 m
Angle of internal friction	0.10
Unit weight of the fill	0.05
Sub grade modulus	0.25

Figure 4 presents the relationship between the characteristic value for the unit weigth (19 kN/m^3) and the student-T distribution used in the MC analysis.

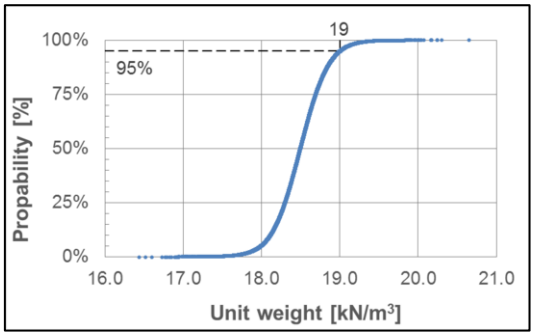

Figure 4. Relationship between characteristic value of the unit weight of the fill properties and the student-T distribution in the MC simulation.

Figure 5 presents the relationship between the characteristic value for the angle of internal friction (45°) and the student-T distribution used in the MC analysis.

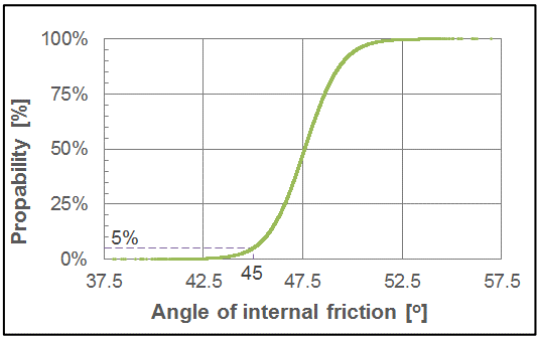

Figure 5. Relationship between characteristic value of the angle of internal friction of the fill and the student-T distribution in the MC simulation.

5.3. Geosynthetic Reinforcement (GR) Properties

5.3.1. Strength

GR suppliers must guarantee the short term design strength of the GR. They are obliged to test the tensile strength for every production batch. Batches are only accepted if all tensile strength results are larger than the strength on the label ($F_{test} > F_{mat}$).

In the MC analysis the variation coefficient V=0.05 is used for the tensile strength F_{mat}, which is a slightly conservative estimate, as the variation provided by the suppliers are somewhat lower.

5.3.2. Time Effects

The tensile strength on the label is the short term strength of the GR leaving the factory. The strength reduces in time mainly due to environmental circumstances, installation damage and material behaviour (creep, relaxation). Designs are based on the strength at the end of the lifetime. Figure 6 presents the reduction in tensile strength with time due to creep for several products (source: BBA certificates). After 100 years the strength is 65% to 75% of the initial strength.

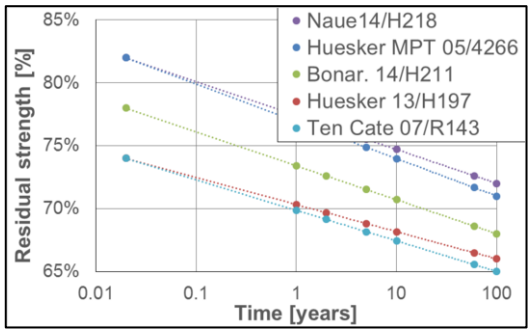

Figure 6. Strength reduction in time due to creep

The tensile strength at the end of the lifetime (100 years) is used for the present calibration study. Analysing the reliability of a system with the tensile strength at the end of its life results in an underestimation of the lifetime reliability.

5.3.3. Strength-strain Relationship

The correlation between tensile strength and axial stiffness is realized in the MC analysis using a ratio factor between the two, with a coefficient of variation of 0.1. Figure 7 illustrates the resulting scatter.

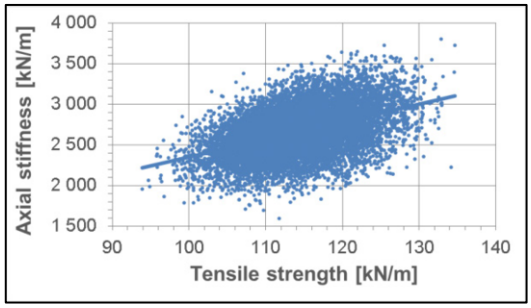

Figure 7. Scatter plot of the correlated relationship between tensile strength and axial stiffness of the GR.

5.4. Loads

The dominant loads in piled embankments are traffic loads. EC1-4 gives characteristic loads. Unfortunately, no appropriate statistical model was available for explicit uncertainty of the traffic load. Instead, the loads applied in the calibrations are nominal values from EC1-4. Since the uncertainty in the load is already accounted for in these nominal values, the target reliability index β was reduced as follows, using

a standardized influence coefficient R = 0.8 for the resistance as suggested by ISO 2394.

$$\beta_{T|s_d} = \Phi(-\alpha_R \beta_T) = \Phi(-0.8\beta_T) \quad (2)$$

Table 3 present the target reliability indices in de ultimate limit state (ULS) for the 3 reliability classes with and without top load.

Table 3. Target reliability index β *ULS*

	RC 1	RC 2	RC 3
Without top load	>3.5	>4.0	>4.6
With top load	>>2.8	>>3.2	>>3.7

For piled embankments, the influence coefficient for the top load (α_r=0.8) may be overestimated. Figure 11 shows that the influence of the external loads on the reliability is much smaller and the factor (α_r) is larger for a thick matress (case 1). For case 1, RC2 without top load (β = 4), the required tensile strength is about 520 kN/m and with top load (β =3.2) about 400 kN/m. Obviously, a smaller tensile strength in the case with top load is not logical and the target reliability index β for the cases with top load $\beta_{T|s_d}$ is used as a bottom limit. Engineering judgement and the calculated reliability index are decisive for the load factor.

6. Step 4: Calibration of the Model Error

6.1. Statistical Characterization

In order to account for the model uncertainty, the definition of the model factor as suggested in Eurocode 0 has been adopted for the design method for piled embankments. The model factor is a combination of the mean bias ($b = r_e/r_t$) and a variation around the mean δ (Eq. (3)), the variation coefficient of which is calculated with Eq. (4).

$$r_e = b \cdot r_t 1 \cdot \delta_i \quad (3)$$

$$V_\delta = \sqrt{e^{s_\Delta^2} - 1} \quad (4)$$

The distribution of δ is assumed lognormal.

The basis for the mean value b and coefficient of variation V is the comparison between calculated and measured strain (r_e and r_t) results, as described in section 4. As the entire data set is not relevant for the envisaged Dutch guidelines, only a subset based on the subgrade modulus was considered. Figure 8 presents the ratio (r_e/r_t) plotted against the subgrade modulus k.

Table 4 shows the model error statistics for different subsets of data in classes with increasing maximum subgrade modulus.

Table 4. Mean bias and variation coefficient of the model error based on subsets of experimental data from Van Eekelen et al. (2015) with different subgrade moduli

subgrade modulus k [kN/m^3]	Number of data sets N	Mean bias b	Coefficient of variation V_δ
0	11	0.833	0.163
≤158	17	0.806	0.246
≤236	*22*	*0.775*	*0.306*
≤480	46	0.679	0.857
≤1200	54	0.700	0.868
≤3138	115	0.727	0.702

In the Netherlands, piled embankments are usually constructed in soft soil areas with large settlements (subgrade modulus k < 236 kN/m^3). Hence, the range of application of the Dutch design guidelines was limited to subgrade moduli up to 240 kN/m^3, which justified using only the 22 experiments reported in the third line of Table 4 with a maximum value of 236 kN/m^3. The model bias for these data is illustrated in Figure 9.

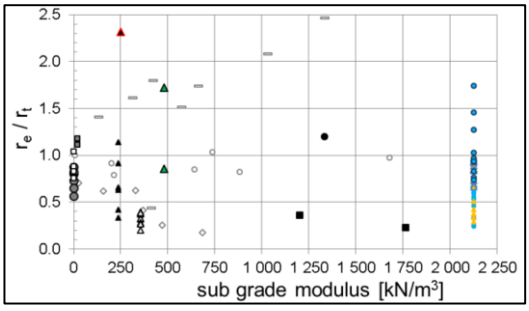

Figure 8. Ratio r_e / r_t versus subgrade modulus k

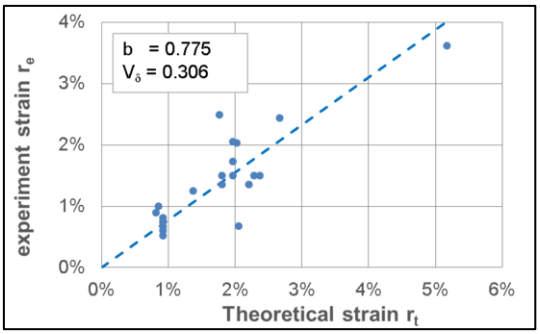

Figure 9. Measured GR strain r_e versus calculated GR strain r_t for the 22 data points from Van Eekelen et al (2015) with subgrade modulus $k < 240$ kN/m^3

6.2. Model Factor (design value)

The dominant failure mechanism in the Serviceability Limit State (SLS) is excessive GR strain. The SLS target reliability index is 2.8, the target probability of failure is 0.24% ($P_f = \Phi(-2.8)$).

Figure 10 shows the results of a MC analysis with the calculated maximum GR strain on the horizontal axis and its probability of exceedance ($P_f(\varepsilon_e < \varepsilon_t)$) on the vertical axis. The calculated maximum strain with all factors equal to 1 was about 2.7%. The 0.24% failure strain was about 3.60 (see figure 9). The model factor is calculated with:

$$\gamma_{model} = \frac{\varepsilon\left(P_f = 0.24\%\right)}{\varepsilon_t} = \frac{3.6}{2.7} \approx 1.4$$

The model factor ensures a safe calculation model with a probability of failure of about 0.24% in the serviceability limit state ($\beta = 2.8$).

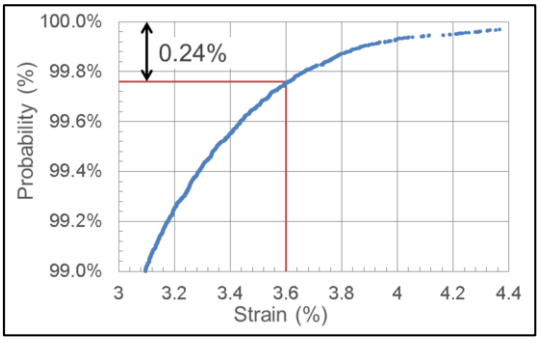

Figure 10. Probability curve of occurrence calculated strains to determine the model factor

7. Step 5: Calibration of the Partial Factors

7.1. Calibration Workflow

The calibration of the partial factors is based on four reference cases that are characteristic for piled embankments in the Netherlands. The partial factors are determined iteratively as shown in the flow chart in Figure 11.

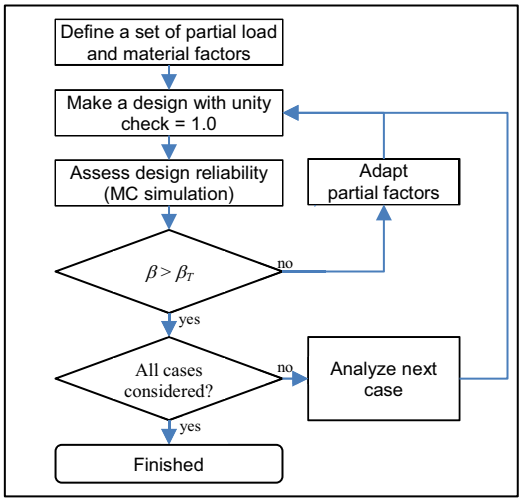

Figure 11. Flow chart of the calibration workflow to determine a set of partial factors which leads to the complying with the target reliability for all test cases

For each test case, data set and set of partial factors, a design is made which meets the unity check for the envisaged design rule. Subsequently, the reliability index of the design is assessed with MC analysis (i.e. the same probability distributions are used for deriving the characteristic values in the design as well as in the reliability analysis) and compared to the target value. The partial factors are amended in an iterative process until all test cases comply with the required reliability index β.

7.2. Analyzed Cases

Table 5 lists the general data of the four cases in the MC-analysis. Case 3 is the common situation for piled embankments. Case 1, 2 and 4 are exceptional situations which represent the limits of the design method.

Table 5. General dimensions of the 4 cases

Case		1	2	3	4
s_x and s_y	[m]	3.25	1.75	2.25	2.25
Height	[m]	10	1.5	3.5	3.5
Squared pile cap	[m]	1.25	0.4	0.75	0.75
Friction angle	[deg]	35	45	45	35
Top load	[kN/m^2]	20	50	20	20

For all cases, the fill unit weight is 19 kN/m^3, square pile caps and pile spacing are applied. The calculations were done for a subgrade modulus of 0 and 100 kN/m^3. The ratio between short term strength and stiffness was 12.

8. Results

8.1. Resulting Safety Factors and Model Factor

Figure 12 presents the relation between the characteristic (95%) long term tensile strength and the calculated reliability index β (markers) for four reference cases.

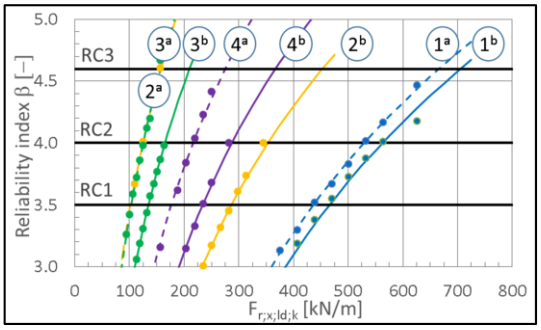

Figure 12. Reliability index – characteristic tensile strength ($F_{r;x;ld;k}$) 4 cases, without top load (^{a}) and with top load (^{b}) and sub grad modulus k = 0 kN/m^3.

The figure shows that the influence of the required tensile strength on the calculated reliability index β is large for thin mattresses (case 2) and small for thick mattresses (case 1).

Table 6 presents the partial factors which comply for all cases with the required reliability and at the same time do not over design the construction. It is not possible to end up with 1 set of partial factors that exactly gives the required reliability for all cases.

Table 6. Resulting partial material- and load factors and the model factor

Partial factor	**RC1**	**RC2**	**RC3**
Required β	**≥ 3.5**	**≥4.0**	**≥ 4.6**
Angle of internal friction	1.05	1.10	1.15
Unit weight	0.95	0.90	0.85
Tensile strength GR	1.30	1.35	1.45
Axial stiffness GR	1.00	1.00	1.00
Subgrade modulus	1.30	1.30	1.30
Top load	1.05	1.10	1.20
Model factor	1.40	1.40	1.40

8.2. Calculated Reliability

Table 7 presents the calculated reliability index β for all 4 cases for the serviceability limit state (SLS) and the 3 reliability classes (RC1, RC2 and RC3) in the ultimate limit state.

Table 7. Calculated reliability index β

Case	Without surcharge load				With surcharge load			
	SLS	RC1	RC2	RC3[1]	SLS	RC1	RC2	RC3[1]
1	2.82	3.56	4.05		2.81	3.58	4.02	
2	***2.67***	***3.31***	***3.67***		*2.63*	*3.28*	***3.65***	
3	2.78	3.50	3.98	4.75	2.76	3.49	3.95	4.31
4	***2.72***	***3.42***	***3.84***		2.70	3.38	3.80	

(1)Due to time not all cases were analysed in RC3 because at least eighty million calculations are required.

In Table 7 the cursive values are a little below the required target reliability index. The situation without surcharge load is not realistic in practice and therefore these relatively low values were accepted.

8.3. Influence of GR stiffness/strength ratio

The ratio between the GR stiffness (J) and the (short term) tensile strength has a limited influence on the calculated reliability β. Table 8 shows this influence.

Table 8. Influence of GR stiffness-strength ratio for case 3

$F_{r;kd;k}$ [kN/m]	$F_{r;ld;k}$ [kN/m]	J [kN/m]	Ratio $J / F_{r;kd;k}$	Reliability index β
178	111	1 260	7	3.53
215	135	2 600	12	3.49
260	163	5 200	20	3.46
542	340	54 000	100	3.42

With an increasing GR stiffness – strength ratio, the reliability index β reduces. The presented partial factors are only applicable for a ratio between strength and stiffness of 7 to 20.

8.4. Non-square piled arrangements: $s_x \neq s_y$

All considered cases so far have a square pile pattern ($s_x = s_y$). Table 9 presents the calculated reliability index β for the case $s_x \neq s_y$ and a surcharge load of 20 kN/m^2.

Table 9. Influence irregular centre to centre distance piles

Case	s_x [m]	s_y [m]	RC1	RC2
3	2.25	2.25	3.49	3.95
	2.00	2.50	3.47	3.90

The influence of the difference between the longitudinal and transversal pile spacing is negligible.

9. Lessons Learned

In the present paper we wanted to share:

- Selection of relevant subsets of experimental data can help in constraining the model uncertainty for a specific application.
- In order to determine which parameters should be factored at all, we successfully followed a sequential approach, meaning that we started with the most influential variables first and then checked one by one if additional factoring seemed efficient and sensible.
- Where very high reliability requirements (e.g. Eurocode RC3) impede the design verification using MC analysis, the partial factors are extrapolated from results of lower reliability (e.g. RC1 and RC2).
- Calibration of partial factors using reliability analysis makes the deliberation process of expert committees objective.
- With 1 set of partial factors it is not possible to design every construction with exactly the required reliability index. The partial factors are focused to design common constructions with the required reliability index in an economical way. For exceptional piled embankments (H < 1.5 m. H > 10 m or J/F > 20) a MC analysis is recommended.

Symbols

$\bar{\Delta}$	$\bar{\Delta} = 1/N \cdot \sum \Delta_i$
Δ_i	$\Delta_i = ln(\delta_i)$
s_Δ^2	Standard variation coefficient of the error term: $s_\Delta^2 = 1/(N-1) \cdot \sum(\Delta_i - \bar{\Delta})^2$
B	Least squares best fit to the ratio between experimental and theoretical results: b=∑re·rt / ∑rt2
N_{fail}	Failure count (R < S)
P_f	Probability of failure ($P_f = \Phi(-\beta)$ = Nfail / N).
r_e	Experiment result. (test result)
r_t	Theoretical results (calculate value)
t_{n-1}^p	Inverse student T distribution for probability p and (n-1) degrees of freedom
V_δ	Variation coefficient error term: $V_\delta = \sqrt{e^{s_\Delta^2} - 1}$
$Z(R\text{-}S)$	Reliability function
δ_i	Error term experiment / theoretical result: rei / (b·rti)
β	Calculated reliability index
$\overline{X}$	Mean value
$F_{r;ld;k}$	Characteristic tensile strength end of the lifetime
$F_{r;kd;k}$	Characteristic tensile strength leaving the factory

References

CUR226, (2015). Ontwerprichtlijn paalmatrassystemen (Dutch Design Guideline Piled Embankments) updated version, to be published in 2015 (in Dutch).

NEN 1990: NEN-EN 1990+A1+A1/C2 (nl), Basis of structural design, ICS 91.010.30; 91.080.01, (December 2011, Eurocode 0).

ISO 2394: (1998). General principles on reliability for structures. ICS 91.080.01

Schweckendiek, T., Vrouwenvelder, A.C.W.M., Calle, E.O.F., Jongejan, R.B., Kanning, W.: Partial Factors for Flood Defenses in the Netherlands. Modern Geotechnical Codes of Practice – Development and Calibration, Fenton, G.A. et al. (eds.). Special Geotechnical Publication. Taylor & Francis. (2013).

Van Duijnen, P.G. Van Eekelen, S.J.M., Van der Stoel, A.E.C., (2010). Monitoring of a railway piled embankment. In: *Proceedings of 9 ICG*, Brazil, 1461-1464.

Van Eekelen, S.J.M., Bezuijen, A., van Tol, A.F., (2013). An analytical model for arching in piled embankments. *Geotextiles and Geomembranes*; 39: 78 - 102.

Van Eekelen, S.J.M., Bezuijen, A., van Tol, A.F., (2015). Validation of analytical models for the design of basal reinforced piled embankments. *Geotextiles and Geomembranes*; 43: 56 - 81.